Signatures of the Chiral Anomaly in Phonon Dynamics

P. Rinkel, P. L. S. Lopes, and Ion Garate
Département de Physique, Institut Quantique and Regroupement Québécois sur les Matériaux de Pointe, Université de Sherbrooke, Sherbrooke, Québec, Canada J1K 2R1

(Received 11 October 2016; revised manuscript received 20 June 2017; published 8 September 2017)

Discovered in high-energy physics, the chiral anomaly has recently made way to materials science by virtue of Weyl semimetals (WSM). Thus far, the main efforts to probe the chiral anomaly in WSM have concentrated on electronic phenomena. Here, we show that the chiral anomaly can have a large impact in the A_1 phonons of enantiomorphic WSM. In these materials, the chiral anomaly produces an unusual magnetic-field-induced resonance in the effective phonon charge, which in turn leads to anomalies in the phonon dispersion, optical reflectivity, and the Raman scattering.

DOI: 10.1103/PhysRevLett.119.107401

Introduction.—A major recent development in quantum materials has been the discovery of three-dimensional Weyl semimetals (WSM) [1]. These materials contain Weyl nodes, i.e., topologically robust points of contact in momentum space between two nondegenerate and linearly dispersing electronic bands. Weyl nodes are characterized by a quantum number called chirality, referring to the parallel or antiparallel locking between momentum and spin. WSM have their low-energy electrodynamics governed by pairs of Weyl nodes with the Hamiltonian

$$\mathcal{H}_W = v\tau^z\boldsymbol{\sigma}\cdot(-i\boldsymbol{\nabla} + e\mathbf{A} + \mathbf{b}\tau^z) + b_0\tau^z - eA_0, \quad (1)$$

where v is the Fermi velocity, τ^z labels the two Weyl nodes of opposite chirality, σ^z labels the two degenerate states at each node, e is the electron's charge, $A^\mu = (eA_0, ev\mathbf{A})$ is the electromagnetic potential, and $b^\mu = (b_0, v\mathbf{b})$ is the axial vector describing the separation between the Weyl nodes in energy and momentum space (b_0 and $\mathbf{b}$, respectively).

A key topological phenomenon in WSM is the chiral anomaly [2], by which collinear electric and magnetic fields ($\mathbf{E}$ and $\mathbf{B}$) induce a transfer of electrons between nodes of opposite chirality. This phenomenon results in an unusual electromagnetic response [1,3,4] captured by the Lagrangian $\mathcal{L}_{\text{ax}} = \theta\mathbf{E}\cdot\mathbf{B}$, where $\theta = \mathbf{b}\cdot\mathbf{r} - b_0 t$ is a nondynamical "axion" field, at position $\mathbf{r}$ and time t. While the chiral anomaly has been probed via electronic transport experiments [5], the observed signatures are not conclusive [6] and further probes, providing complementary understanding of the phenomenon, have been proposed [7–10]. These proposals rely on the development of some type of electronic order (charge or magnetic) or nonequilibrium electronic populations. As of now, such conditions are unmet in real WSM.

Relative to the aforementioned proposals, lattice dynamics is ubiquitous, occurs in equilibrium, and can be accurately measured. Moreover, recent theories have predicted an interplay between lattice vibrations and electronic topology [11–15]. A natural question is then whether one might observe fingerprints of the chiral anomaly in phonon properties. To date, phonon measurements have found no evidence of topological effects in WSM [16], in part due to a scarcity of concrete theoretical ideas on what to measure. The objective of this work is to remedy that problem, predicting clear-cut signatures of the chiral anomaly in phonon dynamics. Our main observation is that the coupling between Weyl fermions and phonons can produce fluctuations in θ, leading to anomaly-induced infrared reflectivity, resonant Raman scattering, and phonon self-energy. We predict that such effects take place in external magnetic fields for A_1 phonons of *enantiomorphic* WSM (materials with broken inversion and mirror symmetries), such as $SrSi_2$ [17], trigonal Se and Te [18], Ag_3BO_3, $TlTe_2O_6$, and Ag_2Se [19].

Lattice dynamics in the absence of electrons.—The physical properties of lattice normal modes can be extracted from their equations of motion [20],

$$M(q_0^2 - \omega_{\mathbf{q}\lambda}^2)v_{\mathbf{q}\lambda}(q_0) = \sqrt{N}\mathbf{Q}^{(0)}_{-\mathbf{q}\lambda}\cdot\mathbf{E}_{\mathbf{q}}(q_0). \quad (2)$$

Here, $v_{\mathbf{q}\lambda}(q_0)$ is the phonon normal mode coordinate with frequency and momenta $(q_0, \mathbf{q})$ and branch $\lambda = 1, \ldots, 3r$ for a lattice with N sites and r atoms in the unit cell; M is the total atomic mass in a unit cell and $\omega_{\mathbf{q}\lambda}$ is the phonon dispersion for branch λ, in the absence of conduction electrons and photons. The right-hand side of Eq. (2) describes a driving force, exerted by the total electric field $\mathbf{E}_{\mathbf{q}}(q_0)$ and proportional to the *mode-effective* phonon charge [20,21]

$$\mathbf{Q}^{(0)}_{\mathbf{q}\lambda} = e\sum_s Z_s e^{-i\mathbf{q}\cdot\mathbf{t}_s}\mathbf{p}_{\mathbf{q}\lambda s}, \quad (3)$$

where s labels the atoms in a unit cell, $\mathbf{t}_s$ is the position of atom s (measured from an origin located at the unit cell), eZ_s is the effective Born charge of atom s (with $\sum_s Z_s = 0$), and $\mathbf{p}_{\mathbf{q}\lambda s}$ is the polarization vector describing the motion of atom s in the phonon mode λ. In the long-wavelength limit, Eq. (3) describes the change in the

intracell electric polarization produced by atomic displacements in mode λ. The modes are classified as infrared (IR) active if $Q^{(0)}_{\mathbf{q}=\mathbf{0}\lambda} \neq 0$ and IR inactive otherwise. All acoustic modes are IR inactive due to $\sum_s Z_s = 0$. When probing the system with visible and IR photons, we can focus on the physics of optical modes at small momenta, for which $\omega_{\mathbf{q}\lambda} \approx \omega_{0,\lambda}$. As we show below, the chiral anomaly of Weyl fermions affects Eq. (2) via a dynamical renormalization of $\mathbf{Q}^{(0)}$.

Electron-phonon interaction.—The departure of the atoms from their equilibrium positions induces a change $\delta U(\mathbf{r}, t)$ in the lattice potential $U(\mathbf{r})$. This couples locally to the electronic density as $\mathcal{H}_{\rm ep} = \int d^3\mathbf{r}\psi^\dagger(\mathbf{r})\psi(\mathbf{r})\delta U(\mathbf{r}, t)$, where $\psi^\dagger$ is an electron creation operator. Focusing on electronic states in the vicinity of Weyl nodes, we have [22]

$$\psi(\mathbf{r}) \simeq \frac{1}{\sqrt{\mathcal{V}}}\sum_\tau e^{i\mathbf{k}_\tau\cdot\mathbf{r}}\sum_{|\mathbf{k}|<\Lambda,\sigma} e^{i\mathbf{k}\cdot\mathbf{r}}u_{\sigma\tau}(\mathbf{r})c_{\mathbf{k}\sigma\tau}, \quad (4)$$

where $\mathcal{V}$ is the sample volume, $\mathbf{k}_\tau$ is the position of node τ in momentum space, $u_{\sigma\tau}(\mathbf{r}) \equiv u_{\mathbf{k}_\tau\sigma}(\mathbf{r})$ is the periodic part of the Bloch wave function at node τ, $\mathbf{k}$ is the momentum measured from a node, and Λ is a high-momentum cutoff (smaller than the internode separation in $\mathbf{k}$ space). Hereafter, we will be interested in long wavelength phonons ($|\mathbf{q}| \ll |\mathbf{k}_\tau - \mathbf{k}_{\tau'}|$ for $\tau \neq \tau'$), which are unable to scatter electrons between different nodes. In this case, the electron-phonon interaction Hamiltonian reads [23]

$$\mathcal{H}_{\rm ep} = \sum_{\mathbf{kq}}\sum_{\sigma\sigma'\tau}\left(\sum_\lambda g^\lambda_{\sigma\sigma',\tau}(\mathbf{q})v_{\mathbf{q}\lambda}(t)\right)c^\dagger_{\mathbf{k}\sigma\tau}c_{\mathbf{k}-\mathbf{q}\sigma'\tau}, \quad (5)$$

where $|\mathbf{k}|, |\mathbf{k}-\mathbf{q}| < \Lambda$ and

$$g^\lambda_{\sigma\sigma',\tau}(\mathbf{q}) = \frac{\sqrt{N}}{\mathcal{V}}\sum_s \mathbf{p}_{\mathbf{q}\lambda s}\cdot\langle u_{\sigma\tau}|e^{-i\mathbf{q}\cdot\mathbf{r}}\frac{\partial U(\mathbf{r}-\mathbf{t}_s)}{\partial\mathbf{t}_s}|u_{\sigma'\tau}\rangle \quad (6)$$

is the electron-phonon coupling. It is useful to decompose Eq. (6) as

$$g^\lambda_{\sigma\sigma',\tau} = g^\lambda_{00}\delta_{\sigma\sigma'} + \mathbf{g}^\lambda_0\cdot\boldsymbol{\sigma}_{\sigma\sigma'} + \tau(g^\lambda_{0z}\delta_{\sigma\sigma'} + \mathbf{g}^\lambda_z\cdot\boldsymbol{\sigma}_{\sigma\sigma'}), \quad (7)$$

where $\boldsymbol{\sigma}$ is a vector of Pauli matrices and $\tau = \pm 1$. The expansion coefficients are explicitly listed in the Supplemental Material [23]. Comparing Eqs. (5) and (7) with Eq. (1), we infer that $c^\mu(\mathbf{q}, t) \equiv \sum_\lambda(g^\lambda_{00}, \mathbf{g}^\lambda_z)v_{\mathbf{q}\lambda}(t)$ and $c^\mu_5(\mathbf{q}, t) \equiv \sum_\lambda(g^\lambda_{0z}, \mathbf{g}^\lambda_0)v_{\mathbf{q}\lambda}(t)$ behave as effective electromagnetic and axial-vector fields acting on electrons (respectively). In particular, $c^\mu_5(\mathbf{q} \simeq 0, t)$ can be interpreted as phonon-induced fluctuations in the energy difference and momentum separation between Weyl nodes of opposite chirality.

While g^λ_{00} is generally allowed by symmetry, $g^\lambda_{0z} \neq 0$ requires $\sum_\tau|u_{\sigma\tau}(\mathbf{r})|^2\tau \neq 0$, which in turn demands a WSM belonging to an enantiomorphic point group. Similarly, $\mathbf{g}^\lambda_z \neq 0$ requires broken time-reversal (TR), inversion and mirror symmetries, while $\mathbf{g}^\lambda_0 \neq 0$ requires breaking of TR symmetry. In enantiomorphic WSM with TR symmetry, pairs of nodes related by TR give additive contributions to g^λ_{0z}.

Phonon dynamics in presence of Weyl fermions.—Weyl fermions modify the phonon equations of motion by means of an effective action

$$S_{\rm int} = -i\ln\det(i\gamma^\mu\partial_\mu - \gamma^\mu a_\mu - \gamma^5\gamma^\mu a_{5\mu}). \quad (8)$$

Here, $\gamma^\mu = (\tau^x, i\tau^y\boldsymbol{\sigma})$ and $\gamma^5 = \tau^z$ are 4×4 Dirac matrices, whereas $a_{5\mu} = b_\mu + c_{5\mu}$ and $a_\mu = A_\mu + c_\mu$ are the total axial-vector and vector fields including the phonon parts. The inclusion of electromagnetic fields in Eq. (8) is essential because we are interested in optical effects produced by phonons.

To evaluate the influence of Weyl fermions in the phonon dynamics, we expand $S_{\rm int} = S_2 + S_3 + \ldots$ in powers of a^μ and a^μ_5. Afterwards, we solve for $\delta S/\delta v_{\mathbf{q}\lambda}(q_0) = 0$, where $S = S^{(0)} + S_{\rm int}$ is the effective action for phonons and $S^{(0)}$ is the bare phonon action [the latter of which yields Eq. (2)]. Explicitly,

$$S_2 = \int_q \Pi_{\mu\nu}(q)[a^\mu(q)a^\nu(-q) + a^\mu_5(q)a^\nu_5(-q)],$$
$$S_3 = \int_{k,k'} T_{\alpha\mu\nu}(k,k')a^\mu(k)a^\nu(k')a^\alpha_5(-k-k'), \quad (9)$$

where $\int_k \equiv \int d^4k/(2\pi)^4$ and $k^\mu = (k_0, v\mathbf{k})$. The absence of terms with an odd number of a^μ is a consequence of assuming zero chemical potential (charge conjugation symmetry). In addition, we take zero temperature and keep terms that are up to second order in $v_{\mathbf{q}\lambda}$ (harmonic approximation).

The effective Lorentz symmetry of Eq. (1), together with gauge invariance, fixes $\Pi_{\mu\nu}(q) = (q_\mu q_\nu - g_{\mu\nu}q^2)\Pi(q^2)$, where $q^2 = q_0^2 - v^2|\mathbf{q}|^2$ and $\Pi(q^2)$ is the polarization function [24]. Although $\Pi(q^2)$ diverges as $1/\log(q^2)$ [8,25] at $q^2 = 0$ ($q_0 = \pm v|\mathbf{q}|$), we find [23] that S_2 does not contribute qualitatively to the phonon dynamics, unlike the contribution from the chiral anomaly.

The chiral anomaly emerges from S_3, through the amplitude $T_{\mu\nu\lambda}$ associated to the "VVA triangle diagram" [26]. This amplitude has been thoroughly studied in high-energy physics [27], though one important caveat in our case is that Weyl fermions and photons have different phase velocities (v and c). Consequently, $k^2 = (c^2 - v^2)|\mathbf{k}|^2 \neq 0$ for real photons. It is helpful to decompose $T_{\alpha\mu\nu}$ into longitudinal and transverse parts [28],

$$T_{\alpha\mu\nu}(k,k') = T^{(l)}_{\alpha\mu\nu}(k,k') + T^{(t)}_{\alpha\mu\nu}(k,k'), \quad (10)$$

such that $q^\alpha T^{(l)}_{\alpha\mu\nu} \neq 0$ and $q^\alpha T^{(t)}_{\alpha\mu\nu} = 0$, where $q = k + k'$. The Ward identities $k^\mu T_{\alpha\mu\nu} = k'^\nu T_{\alpha\mu\nu} = 0$ ensure the gauge invariance of S_3. In particular, the longitudinal part reads

$$T^{(l)}_{\alpha\mu\nu}(k,k') = w_L(q^2) q_\alpha \epsilon_{\mu\nu\rho\sigma} k^\rho k'^\sigma + \mathcal{O}[(k^2 + k'^2)/\Lambda^2], \tag{11}$$

where $\epsilon_{\mu\nu\rho\sigma}$ is the Levi-Civita tensor and $w_L = -i/(2\pi^2 q^2)$. The *infrared* $(1/q^2)$ pole in w_L is the essence of the chiral anomaly. It is independent of the existence of high-energy bands, as well as of the cutoff Λ; it depends on material properties only through the Fermi velocity v hidden in q^2. Also, the chiral anomaly survives under perturbations that break Lorentz invariance (such as nonzero temperature and chemical potential, or disorder), although the $q^2 = 0$ pole gets broadened into a resonance [29].

The transverse amplitude $T^{(t)}$, more complicated, is unrelated to the chiral anomaly, but does contribute to the phonon dynamics and can cancel the $1/q^2$ pole of $T^{(l)}$ in particular kinematic conditions (as when either k^2 or k'^2 are nonzero [28]).

Nevertheless, the analysis becomes simple [23] when the magnetic field contains a constant and uniform part $\mathbf{B}_0$. In this case, $T^{(t)}$ is nonsingular and may be neglected, while $T^{(l)}$ changes Eq. (2) via $\mathbf{E}_\mathbf{q} \to \mathbf{E}_\mathbf{q}(q_0) + \mathbf{E}^{\rm ph}_\mathbf{q}$ and $\mathbf{Q}^{(0)}_{\mathbf{q}\lambda} \to \mathbf{Q}^{(0)}_{\mathbf{q}\lambda} + \delta\mathbf{Q}_{\mathbf{q}\lambda}(q_0)$. Here, $\mathbf{E}^{\rm ph}_\mathbf{q}(q_0) = (i/ev)\sum_\lambda (v\mathbf{q} g_{00} - q_0 \mathbf{g}_z) v_{\mathbf{q}\lambda}$ is an effective electric field related to phonons, whereas

$$\delta\mathbf{Q}_{-\mathbf{q}\lambda}(-q_0) = i\frac{e^2\mathcal{V}}{\pi^2\hbar^2\sqrt{N}}\frac{\mathbf{B}_0}{q^2}(q_0 g^\lambda_{0z} - v\mathbf{q}\cdot\mathbf{g}^\lambda_0) \tag{12}$$

is a phonon effective charge induced by a magnetic field and mediated by Weyl fermions. Equation (12) is the main finding of this work. It can be reinterpreted as a phonon-modulated topological magnetoelectric polarization: $\delta\mathbf{Q}_{\mathbf{q}\lambda} = \partial^2\mathcal{L}_{\rm ax}/(\partial v_{\mathbf{q}\lambda}\partial\mathbf{E}_{-\mathbf{q}})$, where $\mathcal{L}_{\rm ax} = (\theta + \delta\theta_\mathbf{q})\mathbf{E}_{-\mathbf{q}}\cdot\mathbf{B}_0$ and $\delta\theta_\mathbf{q} \propto i\sum_\lambda (q_0 g^\lambda_{0z} - v\mathbf{q}\cdot\mathbf{g}^\lambda_0) v_{\mathbf{q}\lambda}/q^2$ is a phonon-induced axion.

Magnetically induced effective phonon charges are not unique to WSM: they also occur, e.g., in multiferroic materials [30]. Indeed, according to group theory, phonons that are IR inactive at $\mathbf{B}_0 = 0$ may become IR active at $\mathbf{B}_0 \neq 0$, provided that they belong to the direct product of axial and polar irreducible representations (irreps) [31]. What is unique about WSM is the microscopic mechanism for the $\mathbf{B}$-induced IR activity, namely, that $\delta\mathbf{Q}$ originates from axial electron-phonon interactions $(g^\lambda_{0z}, \mathbf{g}^\lambda_0)$ and that it contains a chiral-anomaly-induced *pole* at $q_0 = \pm v|\mathbf{q}|$. It is crucial that the $\mathbf{B}$-field have a nonzero static and uniform component; otherwise, the pole would get canceled by $T^{(t)}$.

Because θ is a pseudoscalar, $\delta\theta_\mathbf{q} = \sum_\lambda (\partial\theta/\partial v_{\mathbf{q}\lambda}) v_{\mathbf{q}\lambda}$ can be nonzero only if at least one of the modes is pseudoscalar. Pseudoscalar phonons transform as $\mathbf{E}\cdot\mathbf{B}$ under proper and improper rotations. Often, Weyl nodes are located at arbitrary points in the Brillouin zone, where the Bloch states transform according to a one dimensional irrep of the translation subgroup. In such case [32], only phonons that transform as the totally symmetric irrep (A_1) couple to Weyl fermions in the long wavelength limit. Moreover, for A_1 phonons to be pseudoscalar, the crystal must lack mirror planes [31]. Hence, we predict that the main effects of the chiral anomaly will manifest themselves in A_1 phonons of enantiomorphic WSM.

In order to assess the observability of our predictions, we estimate δQ. In a TR-symmetric ($\mathbf{b} = \mathbf{g}^\lambda_0 = \mathbf{g}^\lambda_z = 0$) and enantiomorphic ($b_0 \neq 0 \neq g^\lambda_{0z}$) WSM, we have

$$\frac{|\delta Q_\mathbf{q}(q_0)|}{e} \sim \frac{I_0}{\hbar q_0}\frac{q_0^2}{q_0^2 - v^2\mathbf{q}^2}\frac{|\mathbf{B}_0|\mathcal{V}_c/a_B}{\phi_0}\frac{b_0}{W}, \tag{13}$$

where a_B is the Bohr radius, I_0 is a Rydberg, $\mathcal{V}_c$ is the unit cell volume, ϕ_0 is the quantum of flux, and $W \sim O(\Lambda)$ is a characteristic electronic bandwith. In this estimate, we have assumed that the spatial range of $\partial_{\mathbf{t}_s} U(\mathbf{r} - \mathbf{t}_s)$ is about a unit cell, that its magnitude within that range is about I_0/a_B, and that $\sum_\tau \tau |u_{\sigma\tau}|^2 \simeq (b_0/W)\sum_\tau |u_{\sigma\tau}|^2$. For $|\mathbf{B}_0| \sim 1\,\mathrm{T}$, $\mathcal{V}_c \sim 125\ \text{Å}^3$, $I_0/(\hbar q_0) \sim 10^3$ and $b_0/W \sim 0.1$, we have $|\delta Q_\mathbf{q}(q_0)| \sim 0.1e(1 - v^2|\mathbf{q}|^2/q_0^2)^{-1}$, which is not negligible (especially close to resonance). The unusual frequency dependence and momentum dependence of $\delta\mathbf{Q}$ leads to new physical effects that we discuss next.

Phonon dispersion.—In the electrostatic approximation [33], valid for $c|\mathbf{q}| \gg q_0$, phonons produce longitudinal electric fields $\mathbf{E}_\mathbf{q}(q_0) \simeq -(\sqrt{N}/\epsilon_e\mathcal{V})\hat{\mathbf{q}}\sum_\lambda (\mathbf{Q}_{\mathbf{q}\lambda}\cdot\hat{\mathbf{q}}) v_{\mathbf{q}\lambda}(q_0)$, where $\epsilon_e(\mathbf{q}, q_0)$ is the electronic dielectric function for Weyl fermions [23].

For simplicity we consider a time-reversal invariant WSM and assume low carrier concentrations ($\omega_{\rm plasma} \ll \omega_{\mathbf{q}\lambda}$), so that the plasmon-phonon hybridization is unimportant. Also, as an illustration, we consider a single phonon mode: we assume that it is IR inactive at zero magnetic field, but that it couples axially to electrons. The A_1 phonons in $SrSi_2$, Ag_2Se, and CoSi could be candidates for such a mode [31,34].

Inserting $\mathbf{E}$, $\mathbf{E}^{\rm ph}$, and $\delta\mathbf{Q}$ in Eq. (2), we obtain the phonon dispersion from [23]

$$\omega^2_{\mathbf{q}A_1} - q_0^2 + i\kappa g^{A_1}_{00}\mathbf{q}\cdot\delta\mathbf{Q}_{\mathbf{q}A_1}(q_0) + \eta\frac{|\hat{\mathbf{q}}\cdot\delta\mathbf{Q}_{\mathbf{q}A_1}(q_0)|^2}{\epsilon_e} = 0, \tag{14}$$

where $\kappa = \sqrt{N}/(Me)$ and $\eta = N/(M\mathcal{V})$. The solution of this equation is displayed in Fig. 1. When $\mathbf{B}_0\cdot\hat{\mathbf{q}} = 0$, the only solution is $q_0 = \omega_{\mathbf{q}A_1} \simeq \omega_0$ (for long wavelength phonons). As soon as $\mathbf{B}_0\cdot\hat{\mathbf{q}} \neq 0$, a new mode appears due to the anomaly pole, which has quasilinear dispersion. This mode describes particle-hole pairs propagating at the Fermi velocity, and is the analogue of the pseudoscalar

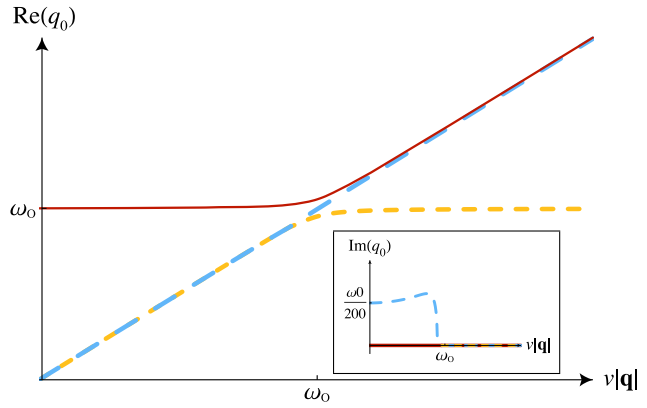

FIG. 1. Anomaly induced coupling between an IR inactive optical phonon and a linearly dispersing pseudoscalar boson in presence of a static and uniform magnetic field $\mathbf{B}_0$, with $\hat{\mathbf{q}} \cdot \mathbf{B}_0 = -1T$ (see Ref. [23] for plots with other values of $\hat{\mathbf{q}} \cdot \mathbf{B}_0$). The curves are solutions to Eq. (14), with parameter values taken from Ref. [23]. When $|\mathbf{q}| \lesssim \omega_0/v$, the linear mode is doubly degenerate but one solution is unstable (antidamped). A large static dielectric constant is assumed so that Landau damping at $q_0 > v|\mathbf{q}|$ can be neglected.

boson discussed in high-energy physics [29,35]. Remarkably, the linear mode couples to the optical phonon in the vicinity of $q_0 \simeq v|\mathbf{q}|$, somewhat like ordinary photons and optical phonons couple in the vicinity of $q_0 \simeq c|\mathbf{q}|$. When $g_{00}^{A_1} = 0$, the gap between the optical phonon and the pseudoscalar boson at $|\mathbf{q}| \simeq \omega_0/v$ scales as $|\hat{\mathbf{q}} \cdot \mathbf{B}_0|^{2/3}$.

Raman scattering.—One-phonon Raman scattering arises from first order corrections to the electronic susceptibility by lattice displacements [36]. The amplitude of Raman scattering can be represented by a triangle diagram with two photon lines and a phonon line.

Let us consider the case where no static magnetic fields are present. In this case, the Raman scattering of a pseudoscalar A_1 phonon is directly linked to Eq. (10) and its contribution to the Raman tensor contains an "axial" component

$$R^{\mathrm{ax}}_{jj'A_1} \propto T_{\alpha\mu\nu}(k,k') \frac{\partial^3[c_5^\alpha(q) A^\mu(k) A^\nu(k')]}{\partial \mathbf{E}_j(k) \partial \mathbf{E}_{j'}(k') \partial v_{\mathbf{q}A_1}(q_0)}, \quad (15)$$

where $j, j' \in \{x, y, z\}$ denote the polarizations of the incoming and scattered electric fields $\mathbf{E}(k)$ and $\mathbf{E}(k')$, respectively, $k = -(\omega, v\mathbf{k})$ and $k' = (\omega', v\mathbf{k}')$ are the momenta of incoming and scattered photons, and $q = k + k' = (q_0, v\mathbf{q})$ is the phonon frequency and momentum. Equation (15) describes the contribution to the Raman tensor coming from phonon modulations of the *magnetoelectric* polarizability. Because k and k' are in the visible [37], the $1/q^2$ pole in $T^{(l)}$ is canceled by $T^{(t)}$. Yet, a weaker singularity remains near $q_0 = v|\mathbf{q}|$ [23],

$$R^{\mathrm{ax}}_{jj'A_1}|_{q^2 \simeq 0} \propto \frac{(q_0 g_{0z} - v\mathbf{q} \cdot \mathbf{g}_0)}{(k^2 - k'^2)^3} \times \left[k^4 \ln\left(\frac{k^2}{q^2}\right) - k'^4 \ln\left(\frac{k'^2}{q^2}\right) \right] \epsilon_{jj'l} (\hat{\mathbf{k}}' - \hat{\mathbf{k}})_l, \quad (16)$$

where $l \in \{x, y, z\}$ and $\epsilon_{jj'l}$ is the Levi-Civita tensor. Aside from being antisymmetric under $j \leftrightarrow j'$, the $\ln(q^2)$ singularity in $R^{\mathrm{ax}}_{jj'\lambda}$ is independent from the ultraviolet cutoff of the theory, i.e., associated to low-energy universal properties of 3D Dirac fermions. This anomaly of the Raman tensor appears experimentally accessible for typical optical phonons, because the momentum $q_0/v \simeq 5 \times 10^5$ cm^{-1} is achievable in the backscattering configuration.

Infrared reflectivity.—Phonon modes with nonzero mode-effective charge produce fluctuating dipole moments that couple to electromagnetic fields. This coupling is quantified by the lattice dielectric susceptibility [20]. Like above, let us consider the case of an A_1 phonon that is IR inactive at zero magnetic field, and couples to electrons axially. This mode's contribution to the lattice susceptibility reads [23]

$$\chi^{\mathrm{latt}}_{jj'}(\mathbf{q}, q_0) = \frac{1}{M\mathcal{V}_c} \frac{\delta Q_{\mathbf{q}\lambda j} \delta Q_{\mathbf{q}\lambda j'}}{\omega^2_{\mathbf{q}\lambda} + i\kappa g^\lambda_{00} \mathbf{q} \cdot \delta \mathbf{Q}_{\mathbf{q}\lambda} - q_0^2}, \quad (17)$$

where $j, j' \in \{x, y, z\}$. Thus, a constant and uniform magnetic field will induce an IR absorption in an otherwise IR inactive mode. In addition, the absorption spectrum depends on $\hat{\mathbf{q}} \cdot \mathbf{B}_0$. This effect can be probed in optical reflectivity experiments [38], e.g., in the following configurations: (i) non-normal incidence of light whose polarization is not parallel to the sample surface, with $\mathbf{B}_0$ along the normal to the surface; (ii) normal incidence of light, whose polarization is parallel to the sample surface, with $\mathbf{B}_0$ parallel to the sample surface. In optical experiments $q_0 = c|\mathbf{q}|$ is fixed and hence the resonance of δQ at $q_0 = v|\mathbf{q}|$ is out of reach. Alternative probes (inelastic x-ray scattering, electron energy loss spectroscopy) may allow us to access the most interesting regime ($q_0 \simeq \omega_{\mathbf{q}\lambda}$ and $|\mathbf{q}| \simeq \omega_{\mathbf{q}\lambda}/v$).

In conclusion, we have predicted a resonant magnetic-field-induced phonon charge as a new fingerprint of the chiral anomaly. This translates into a resonant Raman scattering, a magnetic-field-induced infrared activity, and a peculiar magnetic-field dependence of the dispersion of A_1 phonons in enantiomorphic Weyl semimetals. Although our main results involve optical phonons, anomaly induced effects may be present in the acoustic phonons as well. In addition, the dynamical screening of the electron-phonon interactions, not mentioned above, does not change our results substantially. Further analysis of these issues will be subject of future work.

I. G. acknowledges the hospitality of the Spin Phenomena Interdisciplinary Center (SPICE), where this work was initiated. We have benefited from fruitful discussion with K. Burch, A. Grushin, D. Pesin, B. Roberge. and S. Xu. P. R. and I. G. are funded by the Réseau Québécois des Matériaux de Pointe and the National Research and Engineering Council of Canada. P. L. S. L. is supported by the Canada First Research Excellence Fund.

Note added.—Recently, we noticed work that overlaps with some of our results [39].

[1] For reviews, see, e.g., P. Hosur and X.-L. Qi, C.R. Phys. **14**, 857 (2013); A. A. Burkov, J. Phys. Condens. Matter **27**, 113201 (2015).
[2] K. Fujikawa, Phys. Rev. Lett. **42**, 1195 (1979).
[3] S. A. Parameswaran, T. Grover, D. A. Abanin, D. A. Pesin, and A. Vishwanath, Phys. Rev. X **4**, 031035 (2014).
[4] A. A. Zyuzin and A. A. Burkov, Phys. Rev. B **86**, 115133 (2012).
[5] X. Huang, L. Zhao, Y. Long, P. Wang, D. Chen, Z. Yang, H. Liang, M. Xue, H. Weng, Z. Fang, X. Dai, and G. Chen, Phys. Rev. X **5**, 031023 (2015).
[6] P. Goswami, J. H. Pixley, and S. Das Sarma, Phys. Rev. B **92**, 075205 (2015); R. D. dos Reis, M. O. Ajeesh, N. Kumar, F. Arnold, C. Shekhar, M. Naumann, M. Schmidt, N. Niklas, and E. Hassinger, New J. Phys. **18**, 085006 (2016); F. Arnold, C. Shekhar, S.-C. Wu, Y. Sun, R. D. dos Reis, N. Kumar, M. Naumann, M. O. Ajeesh, M. Schmidt, A. G. Grushin, J. H. Bardarson, M. Baenitz, D. Sokolov, H. Borrmann, M. Nicklas, C. Felser, E. Hassinger, and B. Yan, Nat. Commun. **7**, 11615 (2016).
[7] J. A. Hutasoit, J. Zang, R. Roiban, and C.-X. Liu, Phys. Rev. B **90**, 134409 (2014).
[8] J. Zhou, H.-R. Chang, and D. Xiao, Phys. Rev. B **91**, 035114 (2015).
[9] B. Z. Spivak and A. V. Andreev, Phys. Rev. B **93**, 085107 (2016).
[10] M. D. Redell, S. Mukherjee, and W.-C. Lee, Phys. Rev. B **93**, 241201 (2016).
[11] I. Garate, Phys. Rev. Lett. **110**, 046402 (2013); K. Saha and I. Garate, Phys. Rev. B **89**, 205103 (2014).
[12] K. Saha, K. Légaré, and I. Garate, Phys. Rev. Lett. **115**, 176405 (2015).
[13] H. Shapourian, T. L. Hughes, and S. Ryu, Phys. Rev. B **92**, 165131 (2015).
[14] A. Cortijo, Y. Ferreiros, K. Landsteiner, and M. A. H. Vozmediano, Phys. Rev. Lett. **115**, 177202 (2015).
[15] D. I. Pikulin, A. Chen, and M. Franz, Phys. Rev. X **6**, 041021 (2016).
[16] H. W. Liu, P. Richard, L. X. Zhao, G.-F. Chen, and H. Ding, J. Phys. Condens. Matter **28**, 295401 (2016); B. Xu *et al.*, Nat. Commun. **8**, 14933 (2017).
[17] S.-M. Huang *et al.*, Proc. Natl. Acad. Sci. U.S.A. **113**, 1180 (2016).
[18] M. Hirayama, R. Okugawa, S. Ishibashi, S. Murakami, and T. Miyake, Phys. Rev. Lett. **114**, 206401 (2015).
[19] G. Chang, D. S. Sanchez, B. J. Wieder, S.-Y. Xu, F. Schindler, I. Belopolski, S.-M. Huang, B. Singh, D. Wu, T. Neupert, T.-R. Chang, H. Lin, and M. Z. Hasan, arXiv: 1611.07925.
[20] Yu. A. Il'inskii and L. V. Keldysh, *Electromagnetic Response of Material Media* (Springer, New York, 1984).
[21] X. Gonze and C. Lee, Phys. Rev. B **55**, 10355 (1997).
[22] See, e.g., B. A. Foreman, J. Phys. Condens. Matter **12**, R435 (2000); J. Maciejko and R. Nandkishore, Phys. Rev. B **90**, 035126 (2014).
[23] See Supplemental Material at http://link.aps.org/supplemental/10.1103/PhysRevLett.119.107401 for in-depth discussions regarding the electron-phonon vertices, effective action expansion, the general situation with more than two nodes and the anomalous phonon effective charge.
[24] D. V. Schroeder and M. Peskin, *An Introduction to Quantum Field Theory* (Westview Press, Boulder, CO, 2005).
[25] M. Lv and S.-C. Zhang, Int. J. Mod. Phys. B **27**, 1350177 (2013).
[26] S. L. Adler, Phys. Rev. **177**, 2426 (1969); J. Bell and R. Jackiw, Nuovo Cimento A **60**, 47 (1969).
[27] See, e.g., R. A. Bertlmann, *Anomalies in Quantum Field Theory* (Clarendon Press, Oxford, 1996).
[28] R. Armillis, C. Coriano, L. Delle Rose, and M. Guzzi, J. High Energy Phys. 12 (2009) 029.
[29] H. Itoyama and A. Mueller, Nucl. Phys. **B218**, 349 (1983); A. Gómez Nicola and R. F. Alvarez-Estrada, Int. J. Mod. Phys. A **09**, 1423 (1994); S. D. H. Hsu, F. Sannino, and M. Schwetz, Mod. Phys. Lett. A **16**, 1871 (2001).
[30] J. Vermette, S. Jandl, M. Orlita, and M. M. Gospodinov, Phys. Rev. B **85**, 134445 (2012).
[31] For a review, see, e. g., E. M. Anastassakis, in *Dynamical Properties of Solids*, edited by G. K. Horton and A. A. Maradudin (North-Holland, Amsterdam, 1980), Vol. 4.
[32] R. C. Powell, *Symmetry, Group Theory, and the Physical Properties of Crystals* (Springer, New York, 2010).
[33] M. A. Stroscio and M. Dutta, *Phonons in Nanostructures* (Cambridge University, Cambridge, England, 2004).
[34] M. I. Aroyo, J. M. Perez-Mato, D. Orobengoa, E. Tasci, G. de la Flor, and A. Kirov, Bulg. Chem. Commun. **43**, 183 (2011); M. I. Aroyo, J. M. Perez-Mato, C. Capillas, E. Kroumova, S. Ivantchev, G. Madariaga, A. Kirov, and H. Wondratschek, Z. Kristallogr. **221**, 15 (2006); M. I. Aroyo, A. Kirov, C. Capillas, J. M. Perez-Mato, and H. Wondratschek, Acta Crystallogr. Sect. A **62**, 115 (2006); E. Kroumova, M. I. Aroyo, J. M. Perez-Mato, A. Kirov, C. Capillas, S. Ivantchev, and H. Wondratschek, Phase Transitions **76**, 155 (2003).
[35] M. Giannotti and E. Mottola, Phys. Rev. D **79**, 045014 (2009).
[36] See, e.g., A. Pinczuk and E. Burstein, in *Light Scattering in Solids I*, edited by M. Cardona, Topics in Applied Physics Vol. 50 (Springer, Berlin, 1982).
[37] In real WSM, the frequency of visible photons may be larger than the typical energy scale in which the electronic dispersion can be approximated as linear. Hence, we expect that Eq. (16) will have corrections from high-energy electronic states. Nevertheless, the $\ln(q^2)$ dependence should be robust because it has topological origin.
[38] F. Wooten, Appl. Opt. **23**, 4226 (1984).
[39] Z. Song, J. Zhao, Z. Fang, and X. Dai, Phys. Rev. B **94**, 214306 (2016).